Smart Agricultural Technology 12 (2025) 101470

Contents lists available at ScienceDirect

Smart Agricultural Technology

journal homepage: www.journals.elsevier.com/smart-agricultural-technology

Automated system for extraction of eggshell morphometric characteristics in chicken eggs

Sérgio Luís de Castro Júnior [a,*], Ana Elisa Custódio Montes Cândido [b], Ana Carolina de Sousa Silva [c], Iran José Oliveira da Silva [a]

[a] Environment Livestock Research Group (NUPEA), Department of Biosystems Engineering, "Luiz de Queiroz'' College of Agriculture, University of São Paulo, Piracicaba, São Paulo, Brazil
[b] Regional Research Center of Ribeirão Preto, Institute of Animal Science, Ribeirão Preto, São Paulo, Brazil
[c] Basic Science Department, College of Zootechnics and Food Engineering, University of São Paulo, Pirassununga, Sao Paulo, Brazil

ARTICLE INFO

Keywords:
Computer vision
Egg morphometry
Shell quality
Crack detection
Precision livestock farming

ABSTRACT

The evaluation of eggshell morphometric characteristics is essential to ensure the quality of eggs intended for both consumption and incubation. Conventional methods for this analysis are mostly manual, destructive, time-consuming, and prone to human error. In this context, the present study proposes the development of an automated system based on computer vision for extracting key eggshell features: maximum length and width, area, porosity, and cracks. The system was designed to capture images from two positions, enabling high-resolution analysis of overall egg morphometry and shell porosity. A total of 326 commercial eggs from different production systems were analyzed, including 162 brown-shelled and 164 white-shelled eggs. The results showed a high correlation between the values obtained by the automated system and those from manual measurement methods, with coefficients of determination (R^2) above 0.85 for the morphometric variables. Porosity analysis showed better performance for white-shelled eggs ($R^2 = 0.97$) compared to brown-shelled eggs ($R^2 = 0.87$). Crack detection achieved an accuracy above 90 % for both shell types, demonstrating the effectiveness of the automated method. It is concluded that the proposed system is a promising tool for application in the poultry industry, providing greater efficiency, precision, and reliability in eggshell quality assessment.

1. Introduction

The eggshell represents the outer and visible layer of the egg structure and plays a crucial role in both artificial incubation and the quality of eggs intended for consumption. Therefore, in modern poultry farming, assessing the physical properties of the eggshell is a critical factor in ensuring proper embryonic development and the commercial quality of eggs. Characteristics such as volume, thickness, porosity, and physical integrity directly influence chick hatchability [1,2] and the resistance of eggs to handling and storage [3].

Geometric properties of the egg, such as volume and surface area, have been extensively studied in the context of incubation [4–6]. According to Narushin & Romanov [7], egg size and shape are directly correlated with hatch rates and egg weight. Moreover, larger eggs tend to require longer incubation periods, which affects the operational efficiency of commercial hatcheries [8]. In the commercial egg market, these characteristics are equally relevant, as quality grading is based on egg size and/or weight. Additionally, irregularly shaped eggs are more prone to cracking during transportation and storage [9], directly impacting the profitability of the production chain.

Another essential eggshell feature is its porosity, which enables gas exchange of O_2, CO_2, and water vapor between the external environment and the interior of the egg. This process is fundamental to avian embryonic development during incubation [10] and directly influences shelf life and internal quality of commercial eggs [3,11]. Therefore, understanding the number, size, and distribution of eggshell pores is of great scientific and commercial interest.

Finally, the presence of cracks in the eggshell is another highly relevant aspect for egg handling. Cracked eggs should not be sent to incubation rooms, as they pose a high risk of bacterial contamination, compromising flock health and reducing hatch rates [12]. In the commercial egg market, shell cracks directly affect food safety, as they facilitate microbial invasion, accelerate egg spoilage, and reduce shelf life [13,14].

* Corresponding author.
E-mail address: sergio.castro@usp.br (S.L. Castro Júnior).

https://doi.org/10.1016/j.atech.2025.101470
Received 19 August 2025; Received in revised form 15 September 2025; Accepted 22 September 2025
Available online 22 September 2025

Conventional methods for assessing eggshell properties remain largely manual and often destructive. The Archimedes method, for example, is widely used to estimate egg volume, but it requires immersion in aqueous solution, which interrupts embryogenesis and is thus unfeasible for fertile eggs [5,15]. Likewise, traditional methods for porosity evaluation, such as the use of methylene blue solution [16], present significant operational limitations, as they are time-consuming, rely on chemical reagents, and are subject to human error. The identification of shell cracks—like the other properties mentioned—is prone to failures, since human vision is not naturally adapted to detect microcracks, which often go unnoticed.

On the other hand, the growing demand for efficiency and quality in the poultry industry has driven the adoption of emerging technologies. Concepts such as precision livestock farming, automation, the Internet of Things (IoT), and artificial intelligence are increasingly being explored to optimize egg production and improve poultry system efficiency [17,18]. Among these technologies, computer vision and digital image processing have emerged as promising tools for the non-destructive analysis of eggs [2,19,20].

In this context, the present study aims to develop a computer vision system for the automated analysis of eggshell properties. The system is designed to extract metrics related to geometry, porosity, and structural integrity of the shell, with future potential applications in both hatcheries and the commercial egg industry..

2. Materials and methods

2.1. Experimental samples and variables of interest

The study was conducted in October 2024 under controlled conditions at the facilities of the Environment and Livestock Research Group (Núcleo de Pesquisa em Ambiência) at the University of São Paulo, Brazil. A total of 326 commercial eggs were used, including 162 brown-shelled and 164 white-shelled eggs. The samples were sourced from nine commercial brands, covering three different housing systems (conventional, free-range, and cage-free), and classified into three weight categories commonly adopted by the Brazilian egg industry: large (48–57.99 g), extra (58–67.99 g), and jumbo (over 68 g). Shelf life at the time of analysis ranged from 5 to 19 days. The selection of eggs from various brands and production systems aimed to increase the morphological diversity of the sample set. Before the beginning of the experiment, each egg was randomized, properly cataloged, and evaluated through both the automated assessment system and manual measurements.

The characteristics analyzed included maximum egg length (L), maximum egg width (W), egg surface area (A), shell porosity (p), and crack detection. The development of the unified system followed the typical architecture of computer vision systems, including image acquisition, digital processing of the sample set, object segmentation, and feature extraction (Fig. 1) [2,19].

2.2. Image acquisition

To meet the requirements of this study, a dual image acquisition system was developed. This approach was adopted to enable complete capture of the egg's structure — essential for determining surface area and detecting shell cracks with the egg intact — while porosity analysis required magnified images of specific shell sections, obtained after the eggs were broken. A smartphone (iPhone 13, Apple Inc., United States) equipped with a 12-megapixel camera, wide-angle and ultra-wide lenses, and optical image stabilization was used, mounted on a custom-built platform with vertical movement capability (Fig. 2A). This setup enabled image acquisition in two distinct positions: Position A (Fig. 2B), intended for capturing the entire egg, and Position B (Fig. 2C), designed for detailed analysis of the shell in a magnified area. The camera was positioned 13 cm from the eggs, and a 6x zoom was applied in Position B relative to the image captured in Position A.

To ensure the quality of the resulting image database, the experiment was conducted in a completely dark environment (0 lx of illumination), using a single light source positioned behind the object of interest (eggs). The light source was a commercial candling lamp (Chocmaster, Brazil) with three possible light outputs, depending on the size of the aperture rings. Based on preliminary tests, the medium light intensity (medium ring) was selected, which provided the best contrast between the egg and the background. This approach follows established methodologies, such as those employed by Ma et al. [21], and conventional candling procedures [22].

In Position A, 326 images were acquired, each representing one experimental egg, a sample size consistent with other image processing studies applied to eggs [4,6,23,24]. For porosity analysis (Position B),

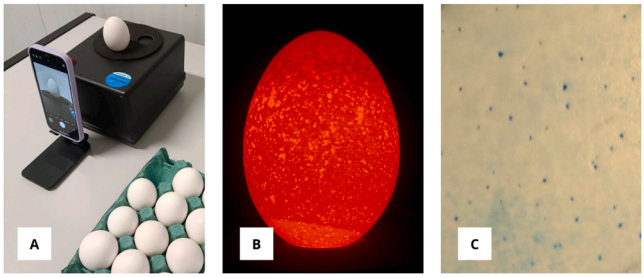

Fig. 2. Image acquisition: System setup (A), example of image captured in Position A, and image captured in Position B (C).

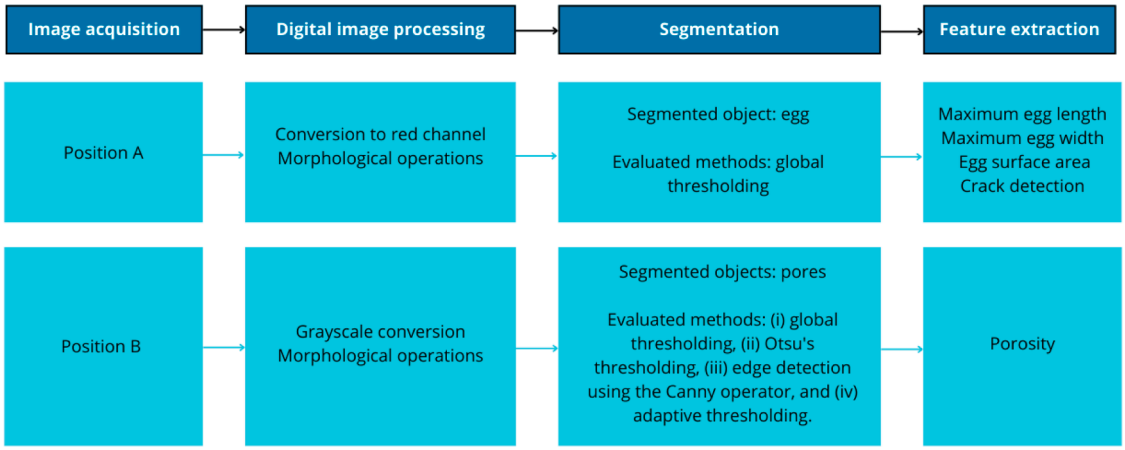

Fig. 1. Flowchart of the automated system for extracting egg morphometric characteristics.

978 images were obtained, as three shell samples were extracted from each experimental egg. This approach is justified by the heterogeneous nature of the shell, given that pore distribution is not uniform across its surface.

2.3. Image processing

Images from Positions A and B were processed in sequential steps aimed at segmentation, morphological operations, and extraction of geometric features [25]. All algorithms were developed in MATLAB® (R2022b, United States).

For Position A, original RGB images were first converted to the red (R) channel, which provided the highest contrast against the dark background and allowed segmentation with a fixed threshold. The threshold value used for binarization was determined empirically through preliminary testing and visual validation. Following the approach adapted from Castro Junior et al. [26], a representative subset of 90 images encompassing a wide range of shell pigmentation patterns and egg morphometric characteristics was analyzed. Threshold levels ranging from 0.30 to 0.80 were systematically applied, and the resulting segmentations were quantitatively compared with manually annotated masks to maximize contrast between the eggshell and the background while minimizing the inclusion of background noise.

After binarization, internal disconnected regions were filled to correct segmentation flaws and ensure the integrity of each object in the image. Morphological processing was then applied to remove noise and standardize shapes, based on mathematical models described by Said & Jambec [27]. This involved four iterations of erosion using a square structuring element (60 pixels per side), reducing segmented region sizes and eliminating small disconnected elements. This was followed by four iterations of dilation using the same structuring element, restoring original dimensions while smoothing edges and removing artifacts.

In contrast, images from Position B were converted to grayscale to remove color information while preserving pixel intensity for subsequent pore analysis. From this grayscale image, segmentation by thresholding was applied. Four different approaches and threshold values were tested: global threshold, Otsu's method, adaptive thresholding, and edge detection, which dynamically adjusts thresholds based on the local intensity distribution of pixels. A representative subset of 90 images encompassing a wide range of shell pigmentation patterns and egg morphometric characteristics was analyzed to benchmark these alternative strategies. The resulting segmentations were quantitatively compared with manually annotated masks using visual assessment and the coefficient of determination (R^2) to evaluate accuracy and robustness. Among the tested methods for pore segmentation, global thresholding combined with noise filtering yielded the best overall performance for both brown-shelled and white-shelled samples, providing the reference baseline for the final pipeline. This procedure produced a binary image in which pixels with intensities above the chosen threshold were assigned to the region of interest (potential pores), whereas the remaining pixels were classified as background (eggshell).

Next, filtering was applied based on the area of objects present in the binary image. Only regions with sizes within a defined range (between 0 and 600 pixels) were retained. This step removed unwanted regions or noise that did not meet the specified size criteria. Additionally, the binary image was inverted before filtering to ensure proper segmentation.

2.4. Feature extraction

With the processed images from Position A, feature extraction was performed on the identified regions. The area of each structure was determined using two complementary approaches. The first relied on direct pixel counting within the segmented binary image, while the second identified the contours of each region and then indexed and labeled the individual structures. From these segmentations, geometric properties—including the area of each object—were extracted.

In addition to area measurements, dimensional information was obtained by generating bounding boxes around the segmented objects and recording their coordinates. These data were used to calculate the height and width of each egg, enabling quantitative analysis of size and shape. The original image was subsequently overlaid with the bounding boxes to visually assess the segmentation and validate the extracted features.

For crack detection, a new predefined intensity threshold was applied following the methodology of Pan et al. [28]. Pixels with values above the threshold were classified as potential pores or anomalies, whereas pixels below the threshold were assigned to the background (eggshell and external field). This binarization highlighted the most relevant regions for detecting structural defects. Candidate regions were then filtered by their geometric perimeter, and only the region with the largest perimeter was retained to ensure that the main structure of interest was analyzed. Finally, the segmented image was fused with the original using a blending method that preserves information from both layers, facilitating visual interpretation and verification of the extracted regions.

For Position B, after size-based filtering, the segmented regions underwent a hole-filling process to correct any internal gaps or discontinuities, followed by a morphological erosion using a 3-pixel square structuring element. This final erosion step smoothed object contours and eliminated small artifacts remaining after binarization. Finally, an object-counting function was applied to the processed binary image to quantify the number of pores present in each shell fragment.

2.5. Validation of the automated system

To validate the system proposed in this study, the results obtained by the automated method were compared with manual readings performed on the same samples. Given the inherent complexity of estimating the surface area of eggs using manual and conventional methods, this study adopted the geometric procedures established by Narushin [29]. As demonstrated by the author, from measurements of the maximum length (L) and maximum width (W) of eggs, it is possible to infer the surface area based on Eqs. (1) and 2, with an estimated error margin of approximately 5 %. The equation used to estimate the egg surface area (A) is expressed as:

$$\textit{Surface area}\ (A) = 3,142 * L^2 * \ n^{-0,532} \tag{1}$$

The dimensionless parameter "n" is determined by Eq. (2):

$$n = 1,057 * \ \left(\frac{L}{W}\right)^{2,372} \tag{2}$$

Where A represents the egg surface area (cm^2); L is the maximum length of the egg (mm); n is the parameter used for calculating A; and W is the maximum width of the egg (mm).

To obtain the variables L and W, manual measurements were taken using a high-precision digital caliper (model 100.174BL, Digimess, Brazil). Manual crack annotations were performed by two trained observers under candling light, in which a bright light is directed through the egg to make shell defects more visible, as described by Wiang and Xiang [30]. A region was labeled as a crack when a continuous linear disruption was clearly visible to the naked eye in the original high-resolution image. Any disagreements between observers were resolved by consensus. Pore counting was conducted according to the methodology described by Rahn et al. [16], where shell fragments were boiled in 5 % NaOH solution, immersed in aqueous solution, dried, and subsequently stained with 1 % methylene blue, facilitating pore quantification under a stereoscopic microscope.

For the comparative analysis between maximum length, maximum width, surface area, and porosity values obtained by the conventional method and those generated by the computer vision system, statistical

regression was employed. A simple linear regression model was used, as applied by Aragua and Mabayo [31] when evaluating egg length and width. For length, width, and area, the coefficient of determination (R^2) and the characteristic equation converting pixel measurements to metric values were obtained. For porosity, R^2, mean absolute error (MAE), regression sum of squares (RSS), error sum of squares (ESS), and total sum of squares (TSS) were extracted.

Additionally, to validate the computer vision system in detecting cracks on the eggshell, the performance of the automated method was analyzed by extracting values of true positives (TP), true negatives (TN), false positives (FP), and false negatives (FN), using the expert manual annotations as the reference standard. From these data, the system's precision (Eq. (3)), recall (Eq. (4)), and F-score (Eq. (5)) metrics were calculated:

$$Precision = \frac{TP}{TP + FP} \tag{3}$$

$$Recall = \frac{TP}{TP + FN} \tag{4}$$

$$F - score = \frac{TP}{TP \ + \ 0,5(FP + FN)} \tag{5}$$

3. Results

3.1. Processing and validation – position A

Starting from a color RGB image (Fig. 3), digital image processing at Position A (PA) began with binarization/thresholding and noise removal. Before the actual binarization, the image was split into its R (red), G (green), and B (blue) channels, with the R channel showing the highest contrast with the background and greater ease of processing. Thus, only the R channel was used in subsequent steps.

It is also important to emphasize the significance of the thresholding step, as it plays a crucial role in the success of the subsequent digital image processing stages. The threshold choice directly influences segmentation quality [32]. A threshold value of 0.60 provided the best results in the proposed method for both white (Fig. 3A) and brown shell samples (Fig. 3B). Thresholds below this value increased visible noise in the image, while thresholds above misclassified object pixels as background.

In some cases, the threshold used during binarization was not fully effective in segmenting the object from the background. Therefore, noise removal processes were necessary to achieve more satisfactory outcomes (Fig. 3.3). The algorithm proved particularly helpful in addressing shadows cast by the eggs on the candling device, which is made of reflective black plastic. Morphological operations were the most effective strategies for eliminating potential background points that, due to lighting, appeared above the threshold during binarization. Such operations are commonly employed in other biologically-focused studies [33,34].

As a result of the digital image processing, morphometric characteristics of the eggs were successfully extracted. Initially, algorithms were used to extract the area (in pixels) of the highlighted object. Concurrently, a representative image was created, coloring the identified area as part of the object (Fig. 3.4). Finally, other algorithms were implemented to extract the maximum length and width of the object. This involved creating a bounding box around the pixels classified as part of the object (Fig. 3.5).

For validation of the automated system, its ability to obtain width, length, and area was compared to manual/conventional measurements. Table 1 summarizes the morphometric shell parameters collected manually: weight, maximum length, and maximum width. The surface

Table 1
Characterization of white and brown eggshell samples.

Parameter	Maximum	Minimum	Mean	Standard Deviation (±)	Coefficient of Variation (%)
		Brown eggs			
Weight P (g)	74.15	45.95	57.00	6.09	10.68
Maximum length L (mm)	63.19	50.42	56.32	2.69	4.78
Maximum width W (mm)	47.83	40.22	43.19	1.48	3.43
Surface area A (cm^2)	82.43	60.83	69.29	5.02	7.24
		White eggs			
Weight P (g)	70.62	35.74	58.74	4.99	8.49
Maximum length L (mm)	63.28	52.62	56.72	2.25	3.97
Maximum width W (mm)	46.67	40.23	43.59	1.29	2.97
Surface area A (cm^2)	82.09	62.26	70.43	4.08	5.80

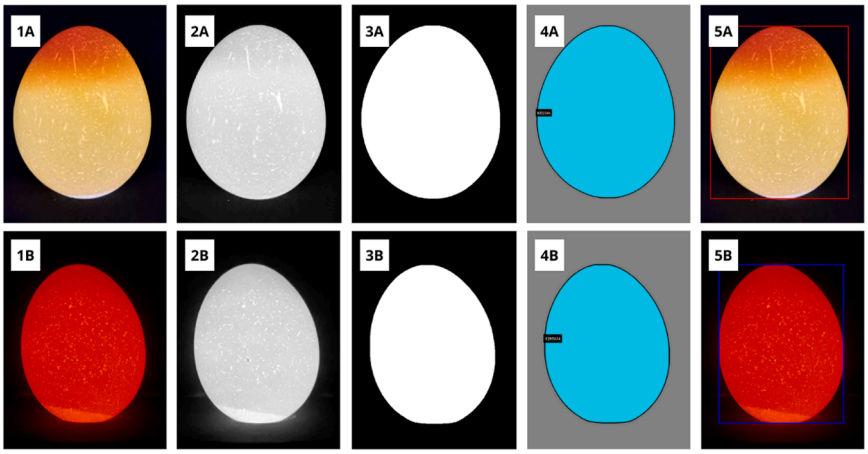

Fig. 3. Stages of digital processing of a white eggshell sample (A) and a brown eggshell (B). 1: original RGB image; 2: image with the R channel; 3: processed and binarized image; 4: visual extraction of area, in pixels; 5: original image overlaid with bounding box for extraction of maximum length and width.

area was calculated using Eqs. (1) and 2.

Table 2 presents the results of the linear regression for the morphometric variables of brown- and white-shelled eggs collected in Position A. The coefficient of determination (R^2) indicates the goodness of fit of the model to the data. R^2 values ranged from 0.8523 to 0.9389, indicating a good fit of the equations. Numerically, white-shelled eggs showed slightly higher R^2 values compared to brown-shelled eggs for all analyzed variables.

Fig. 4 presents the curves obtained from the linear regression analysis used to compare the manual and automated methods. In this analysis, no distinction was made between white and brown eggs, and all samples were analyzed using both the conventional and the proposed methods. The results showed that the coefficient of determination (R^2) reached 0.9303 for the maximum length (Fig. 4A), when comparing real measurements with pixel values obtained through digital processing. For maximum width (Fig. 4B), R^2 was 0.8988, indicating a similar range of variation.

A similar trend was observed for the comparison of surface areas (Fig. 4C), where R^2 reached 0.8382. It is worth noting that while the manual method estimated the area using equations, the digital processing system provided this value directly, simplifying the conventional process.

The crack detection process in eggs (Fig. 5) employed specific digital image processing steps to identify structural imperfections in a non-destructive manner. Initially, the original color image (Fig. 5A) was converted to grayscale (R channel), removing color information and emphasizing intensity variations that could indicate the presence of cracks.

Subsequently, binarization was applied — similar to the previously described steps — converting the image into black and white using a global intensity threshold of 0.12 (Fig. 5C). Pixels with intensity above the threshold were converted to white, while the rest became black, highlighting areas of interest such as cracks and reducing irrelevant information. The next step involved the use of analytical algorithms that identified linear and discontinuous patterns characteristic of cracks, isolating them while discarding noise, pores, or other irrelevant details (Fig. 5D). Finally, the detection results were overlaid onto the original image, making it easier to visualize the location and extent of the cracks (Fig. 5E).

Evaluating the accuracy of a crack detection method in eggs is essential to validate its effectiveness in identifying structural imperfections. Table 3 presents the performance metrics of the proposed system, considering different eggshell colors (brown and white). The analyzed parameters included precision, recall, and F-score, which provide a detailed assessment of the method's ability to correctly identify cracks while minimizing false positives and false negatives.

The results show that the crack detection precision was slightly higher for brown-shelled eggs (96.15 %) compared to white-shelled eggs (91.17 %). This performance may be related to differences in texture or light reflection between the different shell colors. Recall values were similar for both categories, indicating that the method successfully detected most existing cracks, with a slight advantage for brown eggs (89.28 %) over white eggs (88.57 %). The F-score, which combines precision and recall, was also higher for brown eggs (92.59 %) compared to white eggs (89.85 %), reinforcing the trend of better performance for this shell tone. These results suggest that shell color may influence the detection system's response, indicating the need for adjustments to ensure greater consistency in crack identification across different egg types.

Finally, Fig. 6 presents representative failure cases observed during algorithm testing. The first case (Fig. 6A) highlights the effect of heterogeneous shell pigmentation, where a darker patch of the brown shell (at the apical end of the egg) was partially excluded from the segmented area, leading to underestimated length and area measurements. In the second case (Fig. 6B), the egg's low light transmittance (characteristic of a rotten egg) led to a more incomplete segmentation than in the first case, highlighting the system's sensitivity to illumination and the internal properties of the egg. The last case (Fig. 6C) illustrates a false-positive crack detection: a superficial imperfection that allowed greater light passage was misinterpreted as a true crack by the algorithm. These examples emphasize conditions, such as uneven pigmentation, poor light transmission, and surface irregularities, under which the pipeline may fail or produce misjudgments, reinforcing the need for improved lighting control, adaptive thresholding, and additional validation steps to enhance robustness.

Table 2
Regressão linear para as variáveis morfométricas coletadas da Posição A.

Parameter	Shell color	R^2	Characteristic equation
Maximum length	Brown	0.9262	$y = 0.0167x + 3.9135$
	White	0.9389	$y = 0.0182x - 0.9002$
Maximum width	Brown	0.8873	$y = 0.0134x + 10.229$
	White	0.9036	$y = 0.0127x + 12.325$
Surface area	Brown	0.8523	$z = 9E\text{-}06x + 16.449$
	White	0.8807	$z = 9E\text{-}06x + 15.471$

Notes: x indicates the pixel value of the variable; y indicates the variable value in mm; z indicates the variable value in cm^2.

3.2. Processing and validation – position B

Similar to what was done for position A, the images obtained from position B were transformed from RGB images (Fig. 7A) to grayscale and then binarized. Unlike position A, the grayscale channel was found to be the best alternative for proceeding with the processing. Noise filtering and contrast adjustment procedures were required, as also performed in the image processing for position A. It was also observed that adjustments to processing functions were necessary depending on the shell color (white or brown), requiring different threshold values.

To evaluate segmentation performance, a representative subset of 90 images encompassing a wide range of shell pigmentation patterns and egg morphometric characteristics was analyzed. Four methods were tested on this subset: global thresholding (Fig. 7B), Otsu's thresholding (Fig. 7C), adaptive thresholding (Fig. 6D), and edge detection (Fig. 7E). Morphological filters were applied during segmentation to remove noise. Among the tested methods for pore segmentation, global thresholding combined with noise filtering yielded the best result (Fig. 7F) for both brown-shelled samples (threshold = 0.59) and white-shelled samples (threshold = 0.56). Based on this optimal segmentation, feature extraction was performed, and pores were counted using object-counting functions. Table 4 presents the regression model fitting metrics for predicting the number of pores in brown and white eggs. For white-shelled eggs, the R^2 value was 0.972, suggesting that the model explains 97.2 % of the variability in pore number, while for brown-shelled eggs, R^2 was lower (0.872), indicating that the model explains 87.2 % of the variability. This suggests that the regression model is more efficient at predicting pore numbers in white eggs than in brown ones, corroborating results obtained from other metrics, as shown in Table 2.

The mean error (ME) and root mean square error (RMSE) indicate the model's accuracy. The ME and RMSE values were significantly lower for white eggs (ME = 33.863 and RMSE = 5.819) compared to brown eggs (ME = 181.676 and RMSE = 13.478). This indicates that the prediction of pore numbers in white eggs was more accurate, while the model showed higher error for brown eggs. The sum of squares for regression (SSR) represents the variability explained by the model. SSR values were similar for both types of eggs (599,344.0 for brown eggs and 566,364.6 for white eggs). However, the sum of squared errors (SSE) was higher for brown eggs (88,112.94) than for white eggs (16,423.45), highlighting that there is more unexplained variability in the model for brown-shelled eggs. The total sum of squares (SST) reflects the total variability in the number of pores. The higher SST value for brown eggs (687,456.9) compared to white eggs (582,788.0) suggests that the natural variability in pore number is greater in brown eggs.

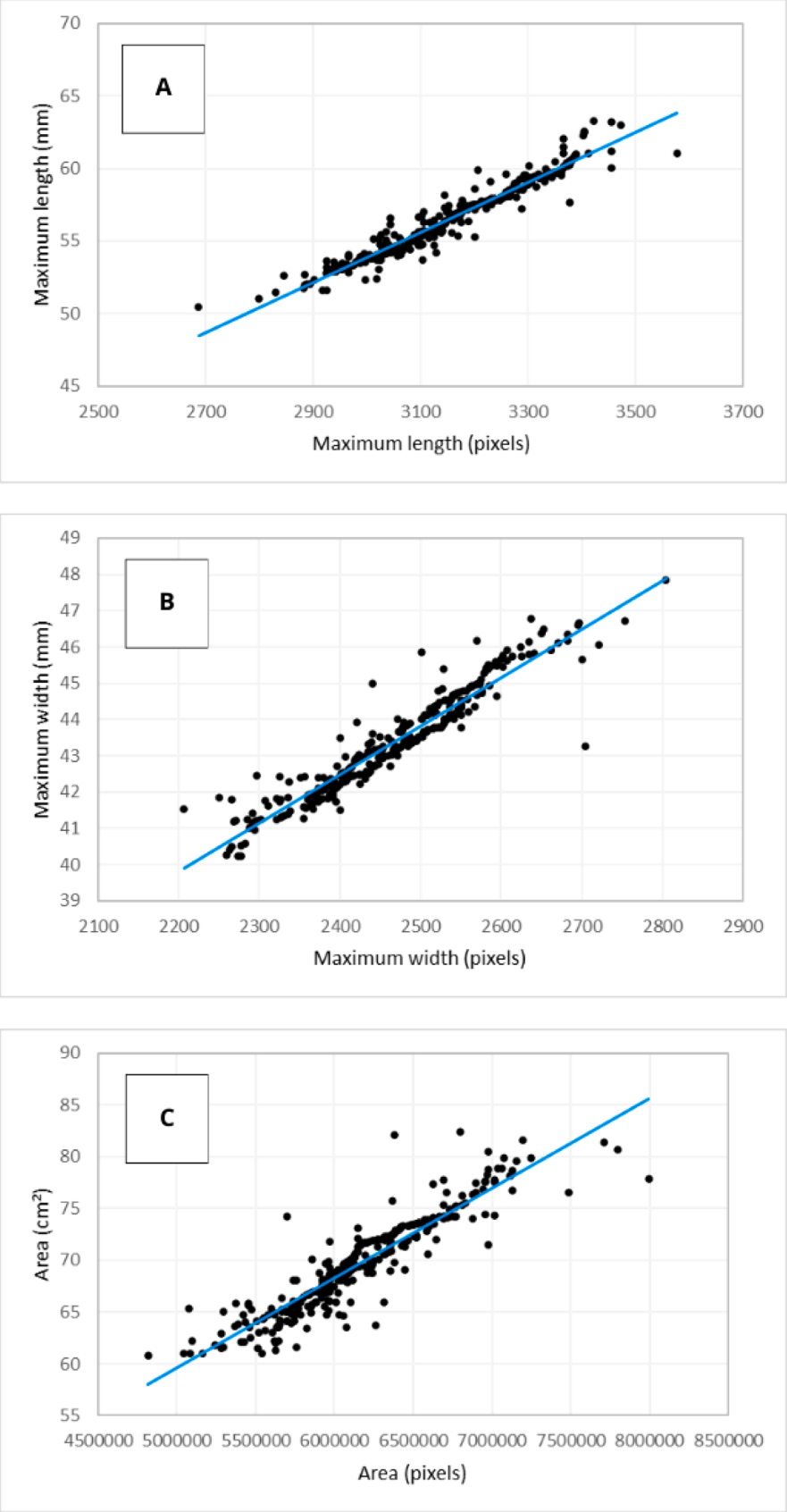

Fig. 4. Scatter plots: Maximum length (A), maximum width (B), and surface area (C).

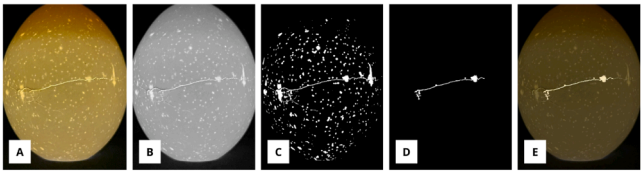

Fig. 5. Stages of digital processing for a white eggshell sample. A: original RGB image; B: image with R channel; C: processed and binarized image; D: visual extraction of the crack; E: original image overlaid with the identified crack.

Table 3
Crack identification metrics for the evaluated eggs.

Evaluation Metrics	Shell Color	
	Brown	White
Precision, %	96.15	91.17
Recall, %	89.28	88.57
f-score, %	92.59	89.85

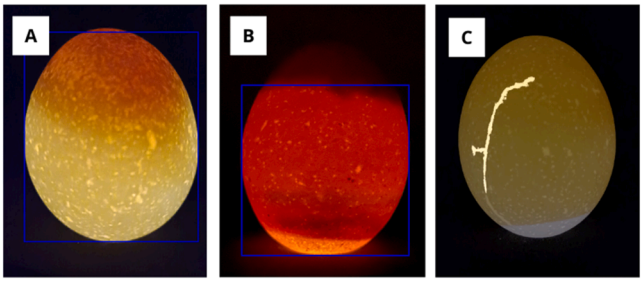

Fig. 6. Representative failure cases of the computer-vision pipeline for eggshell analysis. Case A shows an egg with heterogeneous shell pigmentation, where a darker region was partially excluded from the segmented area. Case B presents a low-transmittance (rotten) egg in which insufficient light penetration prevented proper segmentation. Case C depicts a false-positive crack detection, in which a superficial shell irregularity allowing increased light passage was misclassified as a true crack.

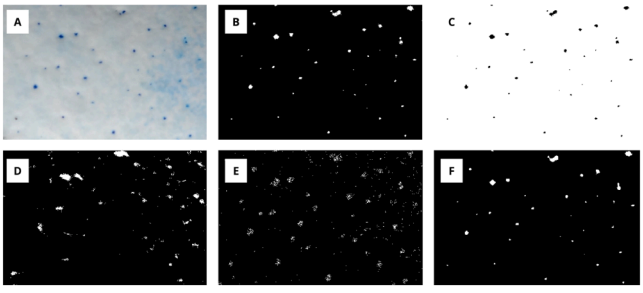

Fig. 7. Digital processing steps for a white eggshell sample. A: original RGB image; B: binarization using global thresholding; C: binarization using Otsu's method; D: binarization using adaptive thresholding; E: binarization using edge detection; F: binarization using global thresholding after morphological operations.

In addition to this analysis, Fig. 8 presents two types of analyses for assessing the number of pores in brown and white eggs: scatter plots (A and C) and Bland-Altman plots (B and D).

The scatter plots (Figs. 8A and 8C) show the relationship between automated and manual measurements of pore count. In both cases, a strong linear correlation was observed, evidenced by the distribution of points along the trend line. However, small variations were noted along the Y-axis, suggesting occasional discrepancies between the measurement methods.

The Bland-Altman plots (Figs. 8B and 8D) provide a more detailed assessment of agreement between the methods, identifying systematic error trends. In these plots, the difference between measurements is plotted against the mean of the measurements. The red dotted lines represent the limits of agreement, within which most observations are expected to lie. Comparing plots B and D, the dispersion of points in plot B is smaller than in plot D, indicating that pore count measurements in white-shelled eggs showed less variation between methods compared to brown-shelled eggs.

These results reinforce the earlier conclusion that pore number prediction in white-shelled eggs shows better model fit and lower mean error compared to brown-shelled eggs. Furthermore, the combined use of scatter plots and Bland-Altman plots provides a robust analysis of the model's accuracy and precision, highlighting the importance of considering additional factors that may influence measurement in different egg types.

4. Discussion

The results obtained in this study demonstrate the feasibility of using computer vision for the automated extraction of eggshell morphometric characteristics. Linear regression analysis revealed coefficients of determination higher than 0.85 for the main morphometric variables extracted by the automated system. However, brown-shelled eggs showed inferior performance in the comparative analysis with the manual method, suggesting lower precision in segmentation and identification of specific structures. In future work, exploring adaptive or hybrid thresholding strategies could further improve the robustness of the segmentation process, particularly when images are acquired under varying illumination conditions.

One of the main reasons for this discrepancy may be attributed to the tonal nuances of brown eggshells, which exhibit greater color variation compared to white eggs. Previous studies indicate that such heterogeneity in pigmentation can hinder binary image segmentation, leading to errors in contour detection and morphological feature extraction [35, 36]. In addition, shadows cast by the candling light source may have been misinterpreted by the algorithm as part of the egg, affecting segmentation accuracy in some analyzed samples. Cunha and Martins [37] suggest that for R^2 values below 0.90, system adjustments are required to improve agreement between methods.

Despite these limitations, system validation demonstrated that the automated method is capable of replacing manual pore count, showing high agreement with values obtained through conventional methods. These findings are consistent with previous studies that used image processing for the characterization of biological structures [19,20].

Regarding the practical application of the proposed system, automated monitoring of egg quality is a key aspect for the poultry industry, both for commercial egg selection and hatchery management. The non-

Table 4
Regression model fitting metrics for predicting the number of pores in eggs.

Parameters	Shell Color	R^2	EM	RQEM	SQR	SQE	SQT
Number of pores	Brown	0.872	181.676	13.478	599,344.0	88,112.94	687,456.9
	White	0.972	33.863	5.819	566,364.6	16,423.45	582,788.0

Notes: R^2 – coefficient of determination; ME – mean error; RMSE – root mean square error; SSR – sum of squares for regression; SSE – sum of squares for error; SST – total sum of squares.

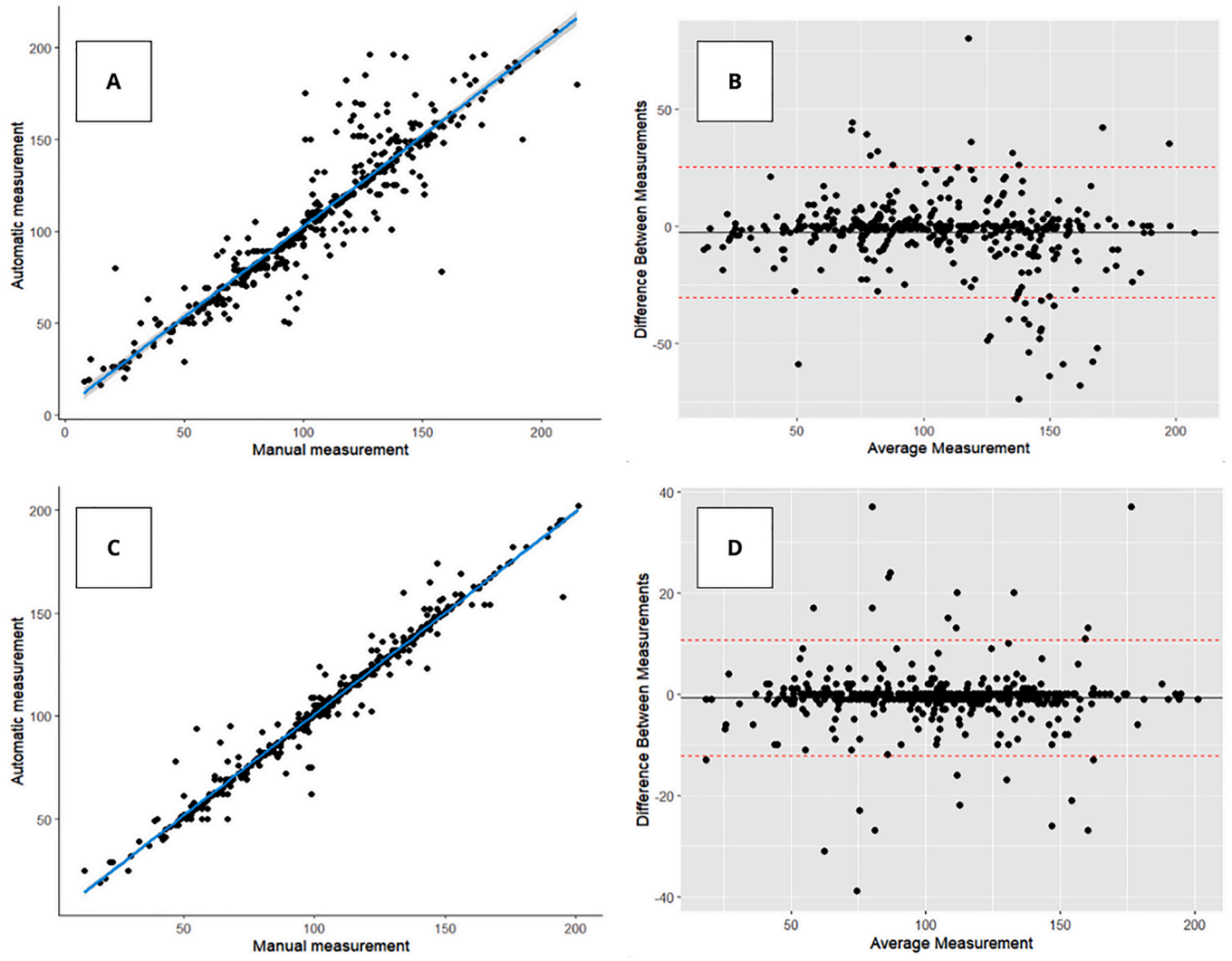

Fig. 8. Scatter plot (A) and Bland-Altman plot (B) for the number of pores in white-shelled eggs. Scatter plot (C) and Bland-Altman plot (D) for the number of pores in brown-shelled eggs.

destructive and automated analysis proposed in this study can be implemented in industrial grading lines to enhance the selection of eggs for consumption, reducing losses associated with cracked or non-standard-sized eggs. However, because porosity assessment requires shell fragments after egg breakage, its direct application to real-time hatchery grading is limited. The system is therefore more suitable for research laboratories or periodic quality-control sampling. Nevertheless, the porosity algorithm remains valuable, as the conventional method is labor-intensive, demands a trained specialist, and relies on chemical reagents, making an automatized approach a faster and more practical alternative.

In hatcheries, eggshell characteristics play a crucial role in embryonic viability, influencing hatchability and chick development [10]. Parameters such as thickness, porosity, and the presence of microcracks can affect gas exchange and increase the risk of bacterial contamination, compromising the quality of the batch [3,11]. The incorporation of automated systems may enable more rigorous control of these factors, improving hatchability rates and reducing losses due to inadequate egg selection for incubation.

Additionally, the proposed system can be integrated with other technologies and precision livestock farming platforms, allowing for real-time data collection and process automation in high-throughput production chains. Such approaches are increasingly being explored in modern poultry farming to optimize operational efficiency and ensure high quality standards [18].

Despite the advances presented in this study, some limitations should be considered. The system's sensitivity to eggshell color variations — particularly in brown eggs — suggests the need for improvements in lighting and algorithm calibration. Future testing may explore the use of deep learning models to enhance segmentation accuracy and microcrack detection, minimizing interference caused by shadows and reflections.

Moreover, more research should expand the sample size and include eggs from different genetic strains, housing systems, and storage periods to assess the robustness of the system under varied conditions. Comparative studies with other imaging techniques may also contribute to improving structural characterization accuracy. In particular, more comprehensive comparisons of thresholding methods should be conducted, especially for images used in pore-count analysis, to ensure optimal segmentation across diverse shell types and lighting conditions. Although the proposed computer vision system achieved high coefficients of determination and strong agreement with manual measurements, the present analysis did not incorporate formal cross-validation or evaluation on an independent dataset. Consequently, some performance metrics may be overestimated due to potential overfitting. Future work should therefore implement k-fold cross-validation or external validation using eggs from diverse production batches and lighting conditions to confirm the generalizability of the segmentation thresholds and regression models, ensuring the robustness

of the system for large-scale industrial deployment.

Finally, the integration of the automated system with IoT devices and cloud-based analytics platforms could enable remote, real-time monitoring of egg quality throughout the production chain. This advancement may establish computer vision as an essential tool for automation and innovation in precision poultry farming, ensuring greater food safety and production efficiency in the egg industry.

In summary, this work demonstrates a practical advance toward fully automated, non-destructive evaluation of eggshell quality by uniting whole-egg morphometry, crack detection, and pore quantification within a single computer-vision pipeline that relies only on low-cost hardware. The system achieved strong agreement with manual measurements ($R^2 > 0.85$ for all key traits) and high crack-detection precision, offering a scalable tool for industrial grading lines and research settings. Nevertheless, important challenges remain: the requirement to fracture shells for porosity analysis limits immediate use in hatcheries or commercial egg grading; brown-shell color heterogeneity and shadow artifacts reduce segmentation accuracy; and the absence of formal cross-validation leaves potential overfitting to be addressed in future work. Tackling these issues, through improved lighting, algorithm calibration, and the adoption of deep learning for more robust segmentation, will be essential for translating the method into routine, high-throughput poultry production.

5. Conclusion

This study presented the development of a computer vision system capable of efficiently analyzing the morphometric characteristics of eggshells, enabling the extraction of features such as length, width, surface area, porosity, and crack detection in a fast, real-time, non-invasive manner, without human interference or the use of chemical reagents. Comparison with manual methods indicated a high correlation for the analyzed morphological variables, although segmentation of brown-shelled eggs posed challenges due to greater color heterogeneity. While the system demonstrated promising results, there are opportunities for improvement, including algorithm adaptations to better handle color and shadow variations, as well as the integration of advanced machine learning techniques. Future research should aim to expand the dataset and validate the technology under different production conditions, establishing computer vision as a key tool for automation in modern poultry farming.

Funding

This work was supported by the São Paulo Research Foundation (FAPESP – 2022/07,442–8) and the Coordination for the Improvement of Higher Education Personnel (CAPES).

Ethical statement

The authors declare that the article entitled *"AUTOMATED SYSTEM FOR EXTRACTION OF EGGSHELL MORPHOMETRIC CHARACTERISTICS IN CHICKEN EGGS"* did not involve the use of live animals or human participants. All data were obtained exclusively from non-fertilized chicken eggs, ensuring that no ethical concerns regarding animal experimentation or human research are applicable to this study.

CRediT authorship contribution statement

Sérgio Luís de Castro Júnior: Writing – review & editing, Writing – original draft, Visualization, Validation, Supervision, Methodology, Investigation, Formal analysis, Data curation, Conceptualization. **Ana Elisa Custódio Montes Cândido:** Visualization, Validation, Methodology, Investigation, Formal analysis, Data curation. **Ana Carolina de Sousa Silva:** Writing – review & editing, Supervision, Software, Methodology, Formal analysis, Conceptualization. **Iran José Oliveira da Silva:** Writing – review & editing, Visualization, Supervision, Resources, Methodology, Funding acquisition, Conceptualization.

Declaration of competing interest

The authors declare the following financial interests/personal relationships which may be considered as potential competing interests:

Iran Jose Oliveira da Silva reports financial support was provided by State of Sao Paulo Research Foundation. If there are other authors, they declare that they have no known competing financial interests or personal relationships that could have appeared to influence the work reported in this paper.

Data availability

Data will be made available on request.

References

[1] S. Batanov, I. Baranova, O. Starostina, E. Shkarupa, The influence of morphological parameters of eggs on the results of incubation, in: BIO Web of Conferences 118, EDP Sciences, 2024 01027.
[2] I. Nyalala, C. Okinda, C. Kunjie, T. Korohou, L. Nyalala, Q. Chao, Weight and volume estimation of poultry and products based on computer vision systems: a review, Poult. Sci. 100 (5) (2021) 101072.
[3] J. Gautron, C. Dombre, F. Nau, C. Feidt, L. Guillier, Production factors affecting the quality of chicken table eggs and egg products in Europe, Animal 16 (2022) 100425.
[4] A.F. Ab Nasir, S.S. Sabarudin, A.P.A. Majeed, A.S.A Ghani, Automated egg grading system using computer vision: investigation on weight measure versus shape parameters, in: IOP Conference Series: Materials Science and Engineering 342, IOP Publishing, 2018 012003.
[5] C. Okinda, Y. Sun, I. Nyalala, T. Korohou, S. Opiyo, J. Wang, M. Shen, Egg volume estimation based on image processing and computer vision, J. Food Eng. 283 (2020) 110041.
[6] M. Soltani, M. Omid, R. Alimardani, Egg volume prediction using machine vision technique based on pappus theorem and artificial neural network, J. Food. Sci. Technol 52 (2015) 3065–3071.
[7] V.G. Narushin, M.N. Romanov, Egg physical characteristics and hatchability, Worlds Poult. Sci. J. 58 (3) (2002) 297–303.
[8] A.M. King'Ori, Review of the factors that influence egg fertility and hatchability in poultry, Int. J. Poult. Sci. 10 (6) (2011) 483–492.
[9] O.K. Chukwuka, I.C. Okoli, N.J. Okeudo, A.B.I. Udedibie, I.P. Ogbuewu, N.O. Aladi, A.A. Omede, Egg quality defects in poultry management and food safety, Asian J. Agricult. Res. 5 (1) (2011) 1–16.
[10] S. Nowaczewski, M. Babuszkiewicz, T. Szablewski, K. Stuper-Szablewska, R. Cegielska-Radziejewska, S. Kaczmarek, M. Hejdysz, Effect of weight and storage time of broiler breeders' eggs on morphology and biochemical features of eggs, embryogenesis, hatchability, and chick quality, Animal 16 (7) (2022) 100564.
[11] K. Wengerska, J. Batkowska, K. Drabik, The eggshell defect as a factor affecting the egg quality after storage, Poult. Sci. 102 (7) (2023) 102749.
[12] B. Guanjun, J. Mimi, X. Yi, C. Shibo, Y. Qinghua, Cracked egg recognition based on machine vision, Comput. Electron. Agricult. 158 (2019) 159–166.
[13] F. Baron, S. Jan, C. Techer, Microbiology of egg and egg products. Handbook of Egg Science and Technology, CRC Press, 2023, pp. 355–396.
[14] J.Y. D'Aoust, Food safety issues and the microbiology of eggs and egg products, Microbiolog. Safe Foods (2009) 187–208.
[15] V.G. Narushin, G. Lu, J. Cugley, M.N. Romanov, D.K. Griffin, A 2-D imaging-assisted geometrical transformation method for non-destructive evaluation of the volume and surface area of avian eggs, Food Control 112 (2020) 107112.
[16] H. Rahn, V.L. Christensen, F.W. Edens, Changes in shell conductance, pores, and physical dimensions of egg and shell during the first breeding cycle of turkey hens, Poult. Sci. 60 (11) (1981) 2536–2541.
[17] V.G. Narushin, N.A. Volkova, A.Y. Dzhagaev, D.K. Griffin, M.N. Romanov, N. A. Zinovieva, Coupling artificial intelligence with proper mathematical algorithms to gain deeper insights into the biology of birds' eggs, Animals 15 (3) (2025) 292.
[18] G. Ren, T. Lin, Y. Ying, G. Chowdhary, K.C. Ting, Agricultural robotics research applicable to poultry production: a review, Comput. Electr. Agricult. 169 (2020) 105216.
[19] N.S.N. Abd Aziz, S.M. Daud, R.A. Dziyauddin, M.Z. Adam, A. Azizan, A review on computer vision technology for monitoring poultry Farm—Application, hardware, and software, IEEE Access 9 (2020) 12431–12445.
[20] X. Yang, R.B. Bist, B. Paneru, T. Liu, T. Applegate, C. Ritz, L. Chai, Computer vision-based cybernetics systems for promoting modern poultry farming: a critical review, Comput. Electron. Agricult. 225 (2024) 109339.
[21] L. Ma, K. Sun, K. Tu, L. Pan, W. Zhang, Identification of double-yolked duck egg using computer vision, PloS one 12 (12) (2017) e0190054.
[22] G.M. Dal'Alba, C. Melek, M. Schneider, G.L. Deolindo, M.M. Boiago, G.A. Faria, D. N. Araujo, In ovo nutrition using honey: effects on hatchability, performance and

carcass yields in broilers, Res., Society Develop. 9 (8) (2020) e43985178-e43985178.
[23] J. Thipakorn, R. Waranusast, P. Riyamongkol, Egg weight prediction and egg size classification using image processing and machine learning, in: 2017 14th International Conference on Electrical Engineering/Electronics, Computer, Telecommunications and Information Technology (ECTI-CON), IEEE, 2017, pp. 477–480.
[24] M.Z. Zalhan, S.S. Syarmila, I.M. Nazri, I.M. Taha, Vision-based egg grade classifier, in: 2016 International Conference on Information and Communication Technology (ICICTM), IEEE, 2016, pp. 31–35.
[25] R.C. Gonzalez, R.E. Woods, Processamento Digital De Imagem, Pearson, 2010. ISBN-10: 8576054019.
[26] S.L. Castro Júnior, A.E.C.M. Cândido, A.C. de Sousa Silva, I.J.O. da Silva, Translucency of chicken eggs: proposal of an automated system for analysis and classification, Poult. Sci. (2025) 105612.
[27] K.A.M. Said, A.B. Jambek, Analysis of image processing using morphological erosion and dilation, J. Phys. 2071 (1) (2021) 012033.
[28] L.Q. Pan, G. Zhan, K. Tu, S. Tu, P. Liu, Eggshell crack detection based on computer vision and acoustic response by means of back-propagation artificial neural network, Europ. Food Res. Technol. 233 (2011) 457–463.
[29] V.G. Narushin, Egg geometry calculation using the measurements of length and breadth, Poult. Sci. 84 (3) (2005) 482–484.
[30] J. Wang, R. Jiang, Eggshell crack detection by dynamic frequency analysis, Europ. Food Res. Technol. 221 (1) (2005) 214–220.
[31] A. Aragua, V.I. Mabayo, A cost-effective approach for chicken egg weight estimation through computer vision, Int. J. Agric. Environ. Food Sci. 2 (3) (2018) 82–87.
[32] V. Wiley, T. Lucas, Computer vision and image processing: a paper review, Int. J. Artific. Intellig. Res. 2 (1) (2018) 29–36.
[33] A. Ghosh, S. Saha, Automatic identification of fracture region within bone in x-ray image, in: 2018 2nd international conference on electronics, materials engineering & nano-technology (IEMENTech), IEEE, 2018, pp. 1–7.
[34] W. Wu, Z. Zhou, S. Wu, Y. Zhang, Automatic liver segmentation on volumetric CT images using supervoxel-based graph cuts, Comput. Math. Methods Med, 2016 (1) (2016) 9093721.
[35] I.B. Barcelos, F.D.C. Belém, L.D.M. João, Z.K.D. Patrocínio Jr, A.X. Falcão, S.J. F Guimarães, A comprehensive review and new taxonomy on superpixel segmentation, ACM Comput. Surv. 56 (8) (2024) 1–39.
[36] A.P. Vartak, V. Mankar, Colour image segmentation-a survey, Int. J. Emerg. Technol. Adv. Eng. 3 (2) (2013) 681–688.
[37] A.R. Cunha, D. Martins, Estudo comparativo entre elementos meteorológicos obtidos em estações meteorológicas convencional e automática em Botucatu, SP, Brasil, Revista Brasileira de Agrometeorologia 12 (1) (2004) 103–111.